

MIXED MODE FRACTURE TOUGHNESS OF STITCHED LAMINATED  
COMPOSITES

By

TOMEK RYS

A THESIS PRESENTED TO THE GRADUATE SCHOOL  
OF THE UNIVERSITY OF FLORIDA IN PARTIAL FULFILLMENT  
OF THE REQUIREMENTS FOR THE DEGREE OF  
MASTER OF SCIENCE

UNIVERSITY OF FLORIDA

2004

Copyright 2004

By

Tomek Rys

## ACKNOWLEDGMENTS

First and foremost I would like to thank my advisor and sponsor, Dr. Bhavani V. Sankar. Without his direct guidance and support the work presented in this thesis would not have been possible. Additionally, I would like to thank my colleagues at the Center for Advanced Composites located on the University of Florida campus. Their support and assistance were invaluable throughout my research.

## TABLE OF CONTENTS

	<u>page</u>
ACKNOWLEDGMENTS .....	iii
LIST OF TABLES .....	vi
LIST OF FIGURES .....	vii
ABSTRACT .....	ix
CHAPTER	
1 INTRODUCTION .....	1
Background Information.....	1
Literature Survey .....	4
Scope of the Thesis.....	5
2 BACKGROUND .....	7
Theory.....	7
Testing of Stitched Composites.....	9
3 EXPERIMENTAL SETUP .....	11
Testing Fixture.....	11
Specimen Preparation .....	14
Experimental Method .....	16
4 FRACTURE TESTS.....	20
Introduction.....	20
Testing and Discussion .....	20
5 FINITE ELEMENT ANALYSIS .....	30
Introduction.....	30
Procedure of Modeling .....	31
Modeling Results.....	33
Crack Propagation Model.....	35

6	CONCLUSIONS .....	38
	Summary .....	38
	Conclusions.....	38
	LIST OF REFERENCES .....	40
	BIOGRAPHICAL SKETCH .....	42

## LIST OF TABLES

<u>Table</u>	<u>page</u>
3-1 Material properties for AS4/3501-6 graphite/epoxy .....	15
3-2 Variation in thickness of each layer in the stacking sequence .....	15
4-1 Average apparent fracture toughness of low-density stitched specimens .....	21
4-2 Average apparent fracture toughness of high-density stitched specimens .....	21
5-1 FE parent and effective fracture toughness .....	33
5-2 Stress intensity factors at crack tip .....	35
5-3 Global versus local mode-mixity ratios .....	35
5-4 Data needed to simulate crack propagation .....	36

## LIST OF FIGURES

<u>Figure</u>	<u>page</u>
1-1 Stitching and Z-pinning of a laminate.....	3
1-2 Stitching Types: (a) Lock stitch, (b) Modified Lock stitch, (c) Chain stitch .....	4
2-1 DCB specimen geometry .....	8
2-2 Modes of Fracture. From left to right: Mode I, Mode II, Mode III.....	9
2-3 Stitched specimen showing failure due to bending moment.....	10
3-1 Mixed Mode testing fixture.....	11
3-2 Free body diagram (FBD) of specimen showing horizontal and vertical force components.....	12
3-3 Grip and specimen ends showing machined arcs used for attachment .....	13
3-4 Mixed Mode fixture showing counterbalance weight for balancing of mechanism prior to testing .....	14
3-5 Specimens showing stitch densities and pre-crack lengths.....	16
3-6 Load versus crosshead displacement plot for a stitched specimen .....	17
3-7 Stitched DCB specimen undergoing testing.....	18
3-8 Schematic of forces for strength of material calculations .....	19
4-1 Fracture toughness versus mode-mixity over entire Mode I to Mode II range.....	22
4-2 Mode I loading: low density specimens, load vs. crosshead displacement.....	23
4-3 Mixed Mode 1 loading: low density specimens, load vs. crosshead displacement .	24
4-4 Mixed Mode 2 loading: low density specimens, load vs. crosshead displacement .	25
4-5 Mixed Mode 3 loading: low density specimens, load vs. crosshead displacement .	26
4-6 Mode I loading: high density specimens, load vs. crosshead displacement .....	27

4-7	Mixed Mode 1 loading: high density specimens, load vs. crosshead displacement	28
4-8	Mixed Mode 2 loading: high density specimens, load vs. crosshead displacement	28
4-9	Mixed Mode 3 loading: high density specimens, load vs. crosshead displacement	29
5-1	2D FE model of fixture and laminate.....	32
5-2	FE model showing crack tip and stitches including the stitch bridging distance.....	32
5-3	Strain energy release rate versus J-Integral contour number .....	34
5-4	Crack propagation model showing first stitch failure .....	37

Abstract of Thesis Presented to the Graduate School  
of the University of Florida in Partial Fulfillment of the  
Requirements for the Degree of Master of Science

MIXED MODE FRACTURE TOUGHNESS OF LAMINATED STITCHED  
COMPOSITES

By

Tomek Rys

August 2004

Chair: Bhavani V. Sankar

Cochair: Peter G. Ifju

Major Department: Mechanical and Aerospace Engineering

The research presented in this thesis is an effort to better understand the failure phenomenon in laminated composites that are reinforced through their thickness with stitches. Through-the-thickness stitching is a method that increases translaminar strength while at the same time preventing crack propagation. A novel test fixture was developed to measure mixed mode fracture toughness under combined Mode I and Mode II loadings.

In addition, a finite element (FEM) model has been created which allows for the prediction of the apparent fracture toughness of various stitched laminates under mixed mode loadings. In the FEM model, the material properties of the laminate, including the stitch material, stitching density, and stitch diameter, can be varied in order to quickly evaluate the sensitivity of fracture toughness with respect to these parameters.

## CHAPTER 1 INTRODUCTION

### **Background Information**

Composite materials have many advantages over conventional materials in aerospace and other applications where the strength to weight ratio is a critical factor. Graphite/epoxy laminated composites have high stiffness-to-weight and strength-to-weight ratios that make them suitable for structural applications. Additionally, composite materials can be tailored to obtain specific properties in various directions and the overall thickness and lay-up of the composite can be optimized for given loading conditions. Composites offer many other advantages over conventional materials including but not limited to: high corrosion resistance, high energy absorption, low thermal expansion, good thermal insulation and electrical resistivity.

Despite all these advantages, graphite/epoxy composite production volumes have not increased drastically in recent years. This stems from two major deficiencies of composite materials. The first being the high material cost and slow manufacturing time of graphite/epoxy composites compared to conventional structural materials. The second major deficiency is the poor inter-laminar strength, fracture toughness and low impact resistance and damage tolerance that composites typically possess.

The properties of these composite laminates depend highly on the fiber orientation and the fiber volume ratio. The strength in the translaminar (through-thickness) direction tends to be significantly smaller than in the fiber direction. For example, the tensile strength of graphite/epoxy laminates is approximately 72 to 116 ksi (500 to 800 MPa) in

the fiber direction while in the translaminar direction the strength is around 2.9 to 4.3 ksi (20 to 30 MPa). This is due to the fact that the load is being predominately carried by the resin matrix, making the composite susceptible to delamination. This delamination is typically an interface crack or a debonded zone between two adjacent layers. This delamination can be initiated by imperfect manufacture or during the impact of a foreign body during service. Typically this delamination is located within the composite and cannot be detected through visual inspection. This initial delamination (crack) can grow rapidly under subsequent application of external load. This can lead to either catastrophic failure of the structure and/or a significant decrease in the load carrying capability. The poor translaminar strength of graphite/epoxy laminates has limited the number of aerospace applications.

Many methods have been developed to improve the translaminar strength and decrease the occurrence of delamination. These methods include the introduction of translaminar reinforcements (TLR) into the composite. TLR can either be of the continuous or discontinuous form. Continuous weaving, knitting, braiding, threads, yarns and tows can be inserted into the laminated using industrial sewing/stitching technology. Discontinuous reinforcements such as short fibers, whiskers and pins can also be inserted into a composite to increase the translaminar strength. Refer to Figure 1-1.

3D weaving, braiding and knitting improve the translaminar strength due to the increased number of fibers in the out of plane direction. The major downfall of these TLR are the large resin pockets that are introduced during manufacture and the reduced number of fibers in the in plane direction. This can lead to reduced in-plane properties. The stitching process differentiates itself by having the stitch as a non-integral part of the

laminate. The stitch is inserted into a 2D preform as a secondary process after lay-up but before the introduction of the resin and subsequent curing. By using stitches as a TLR, the onset of large resin pockets is reduced, especially when compared to 3D weaving. Stitching is one of the most common techniques used to suppress delamination.

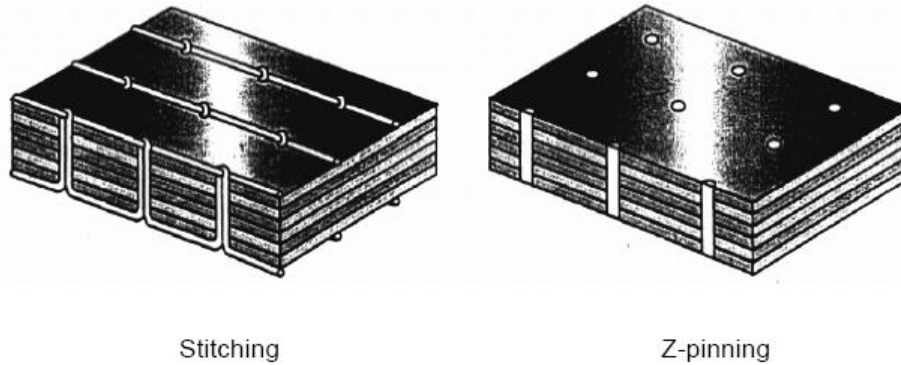


Figure 1-1: Stitching and Z-pinning of a laminate

Composites can be stitched either as preregs (resin impregnated fabrics) or preforms (resin free fabrics). Unfortunately considerable fiber damage occurs when stitching prepreg laminates. This reduces the in plane fiber properties of the composite. Alternatively, stitching of the preform can be done without causing as much fiber damage due to the ability to pull a needle through the resin free fabric.

One of the most critical factors in stitching a laminated composite is the type of stitch used. One of the most common types of stitches is known as the lock stitch. It consists of a two thread loop between the needle and the bobbin threads. The lock stitch requires access to both top and bottom of the laminate. This stitch is used in the apparel industry due to its aesthetic appeal. The intersection of the bobbin and needle threads is concealed in the fabric. This is not favorable for stitching composites because the thread intersection in the middle of the laminate would cause a stress concentration. Therefore,

when stitching composites a modified lock stitch is typically used that allows the needle thread to travel along the surface of the composite rather than in the middle of it.

Additionally, a chain stitch can be used that has a similar mechanism to that of the lock stitch. Figure 1-2 shows all three stitch types discussed above.

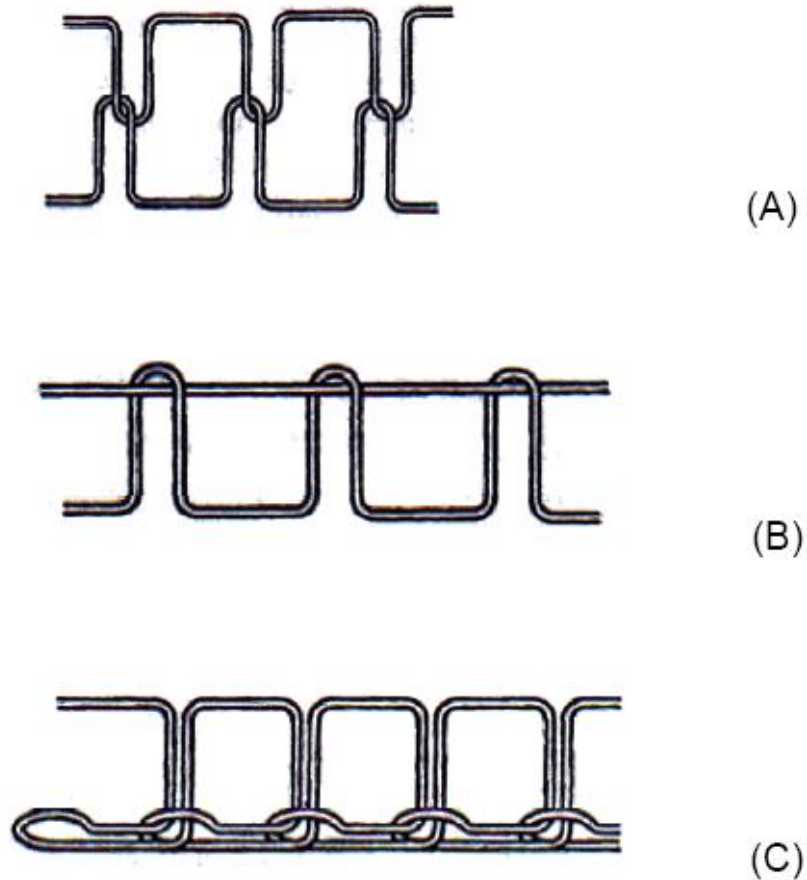


Figure 1-2: Stitching Types: (a) Lock stitch, (b) Modified Lock stitch, (c) Chain stitch

### Literature Survey

Mignery et al. [1] investigated the use of stitching using Kevlar yarn to suppress delamination in graphite/epoxy laminates. Results showed that stitching was an effective suppressant of delamination. In addition, Dexter and Funk [2] investigated the Mode I

fracture toughness of laminates reinforced with Kevlar stitches. Results showed that the fracture toughness increased 30 fold when compared to the unstitched laminate.

Currently, the double cantilever beam (DCB) test is used to determine the Mode I fracture toughness of unstitched composite laminates. In practical applications it is rare to encounter pure Mode I or Mode II loadings. Typical loads are comprised of a combination of both Mode I and Mode II loads referred to as a mixed mode loading condition. Richards and Korjakin [3] used the traditional mixed mode setup to test the fracture toughness of unstitched laminated composites. In their experiments the ratio of Mode I to Mode II was fixed at 1.33 according to linear beam analysis. Reeder and Crews [4-5] developed a new mixed mode experimental setup that simultaneously created a Mode I and Mode II bending load on the specimen from a single applied load. This setup allowed for numerous mixed mode ratios to be tested. Although many researchers have used different approaches to investigate the delamination fracture toughness of composites including mixed mode fracture properties of composites, none have successfully tested the mixed mode fracture toughness of composites with dense translaminar reinforcement. The standard DCB test is not suitable for testing stitched laminates. Typically during the standard DCB test the specimen fails due to high compressive stresses caused by the large bending moment at the crack tip. Due to these problems with the standard DCB test a novel test fixture has been developed by Chen et al. [6] for stitched composites.

### **Scope of the Thesis**

Due to the lack of transverse strength, composite materials are vulnerable to delamination which is either an interface crack or a debond between two adjacent layers. This delamination is typically not detectable by visual inspection of a composite's outer

surfaces. This delamination can be initiated during imperfect manufacture or simply caused by impact of a foreign body during service.

Methods to improve this translaminar strength include stitching. The stitching process improves the apparent fracture toughness of the laminated composite. The aim of the current study is to accurately measure the increase in the fracture toughness incurred by the addition of stitches, and to investigate the effect of various ratios of fracture modes on the composite's fracture toughness.

## CHAPTER 2 BACKGROUND

### Theory

There are two main approaches to analyzing the fracture toughness of a given material: the energy approach and the stress intensity factor approach. Both are commonly used. The energy approach was used during this research due to its ease of adaptability to experimental work. The energy approach states that a crack will only propagate when the energy provided for crack growth is sufficient to overcome the resistance of the material [7]. The material resistance includes but is not limited to the surface energy, plastic work, or any other type of energy dissipation associated with crack propagation [7]. The energy release rate ( $G$ ) is defined as the rate of change in potential energy with crack area. At the onset of crack propagation, the energy release rate is defined as the critical energy release rate, which provides a measure of fracture toughness [7].

For a double cantilever beam (DCB) specimen (Figure 2-1), the Mode I fracture toughness can be found as

$$G_{IC} = \frac{F_C^2 a^2}{bEI} \quad (2-1)$$

where  $F_C$  is the load at which the crack propagation occurs,  $a$  is the current crack length,  $b$  is the width of the specimen and  $EI$  is the equivalent flexural rigidity of the specimen.

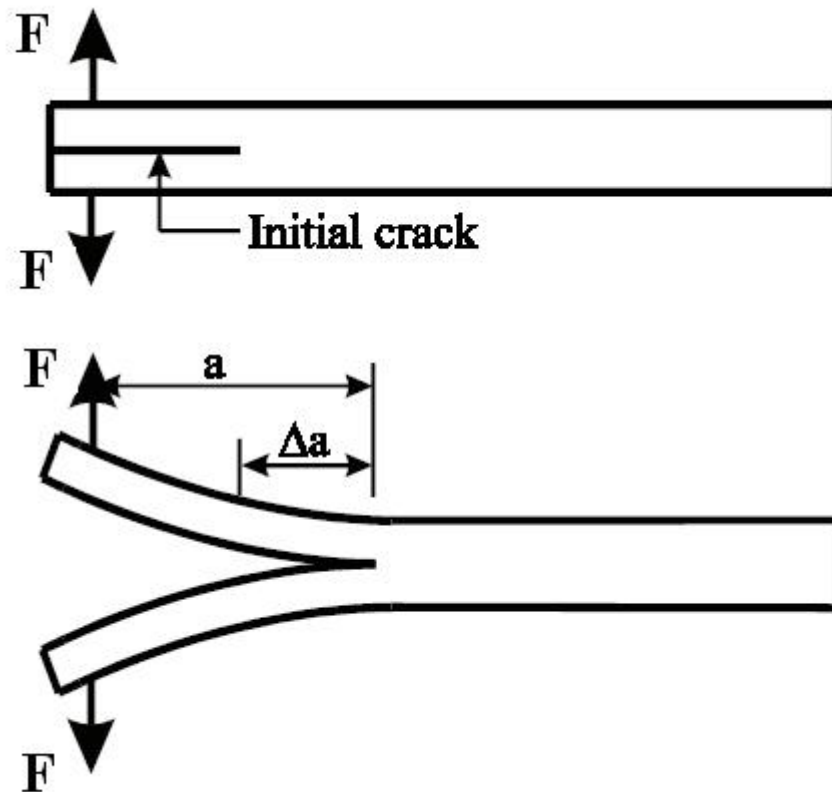


Figure 2-1: DCB specimen geometry

The fracture toughness of stitched laminated composites can be broken into two subcategories.  $G_{\text{parent}}$  is the fracture toughness of the parent material and is constant throughout a structure for a given loading mode. Modes of loading are discussed below. The parent material can be defined as the material which contains the stitches. Alternatively,  $G_{\text{eff}}$  is the fracture toughness related to the parent material but also dependent on the properties of the stitches.

In basic fracture mechanics there are three loading modes: Mode I, Mode II and Mode III. Figure 2-2 shows examples of how each mode is loaded. Mode I is dominated by an opening load, Mode II is dominated by an in plane shearing load, and Mode III is dominated by an out of plane shear.

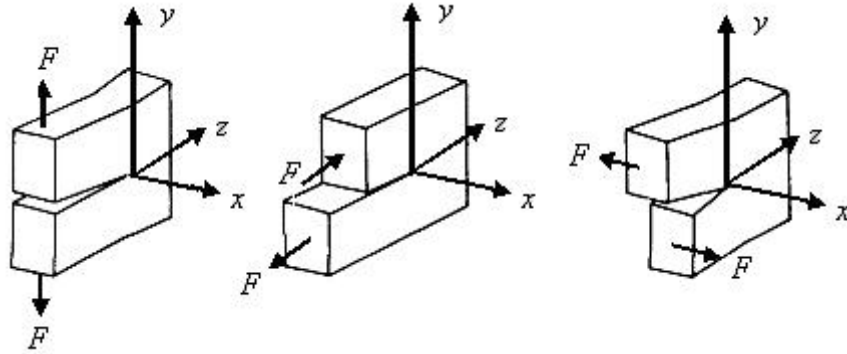


Figure 2-2: Modes of Fracture. From left to right: Mode I, Mode II, Mode III

Typically in real world applications a crack propagates under a combination of these loading conditions. Mixed-mode loading in this research is defined as some combination of Mode I and Mode II loading conditions. Mixed-mode conditions are quantified by a mode-mixity phase angle ( $\psi$ ) (Equation 2-2), which is  $0^\circ$  for pure mode I and  $90^\circ$  for pure mode II. Understanding the mode-mixity of a loading condition is important because of its effects on crack propagation.

$$\psi = \tan^{-1} \left( \frac{G_{II}}{G_I} \right) \quad (2-2)$$

A crack in pure mode II loading commonly requires several times as much energy to initiate crack propagation as compared to a crack propagated under pure mode I loading [7]. Therefore, it becomes necessary to identify the mode-mixity of an experimental setup in order to thoroughly understand results.

### Testing of Stitched Composites

Currently the DCB test as described above is used to measure the Mode I fracture toughness of laminated composites. This method works well for specimens that do not contain translaminar reinforcements. The standard DCB test is not suitable for laminated composites that contain stitches as through the thickness reinforcements. The main reason for this is that the strength of the stitches is very high and a large amount of force

is required to either break them or cause pullout. As the load is increased in the standard DCB test the specimen arms are subjected to large bending moments Figure 2-3. This moment causes the specimen arms to fail due to buckling on the compression side of the arm before crack propagation can be initiated

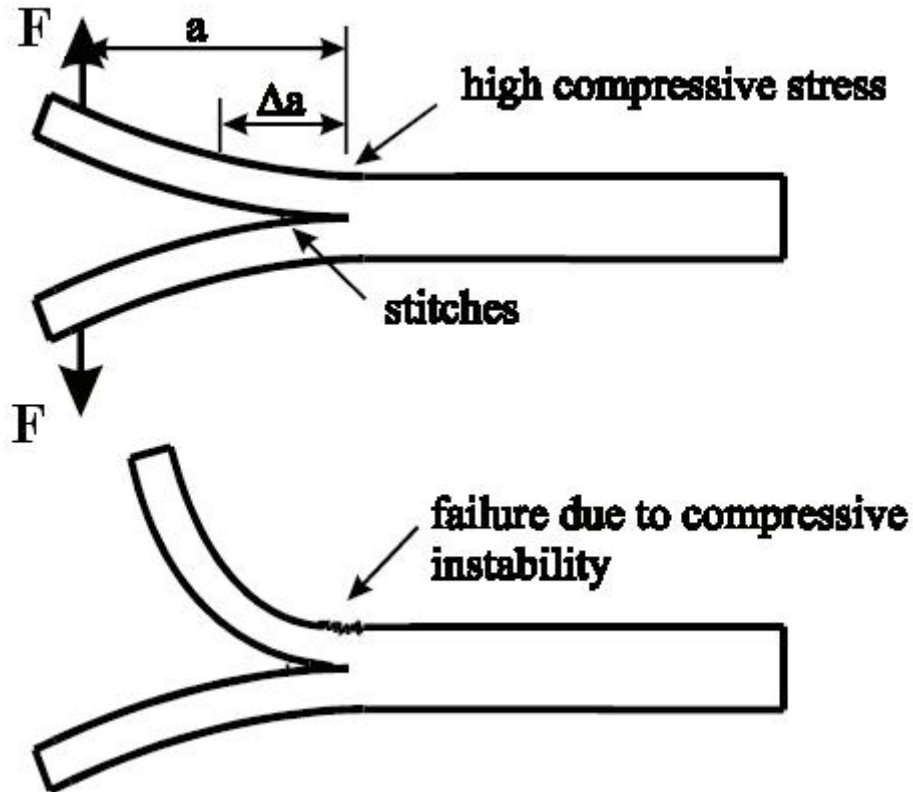


Figure 2-3: Stitched specimen showing failure due to bending moment

Much research has been conducted in investigating new fixtures for testing the fracture toughness of stitched composites. The main focus has been on reducing the aforementioned compressive failure. To effectively eliminate this failure the maximum compressive stress must be reduced. A novel testing fixture has been developed at the University of Florida that incorporates an additional tensile force to neutralize the maximum compressive stress. This fixture is further discussed in Chapter 3.

CHAPTER 3  
EXPERIMENTAL SETUP

**Testing Fixture**

The standard DCB is not suitable for testing stitched composites due to high compressive stresses that cause the specimen to fail before the crack propagation can be initiated. A novel test fixture has been developed to allow for the testing of the fracture toughness of stitched composites. The novel fixture incorporates a horizontal bar that has a series of holes corresponding to numerous mixed mode ratios (Figure 3-1).

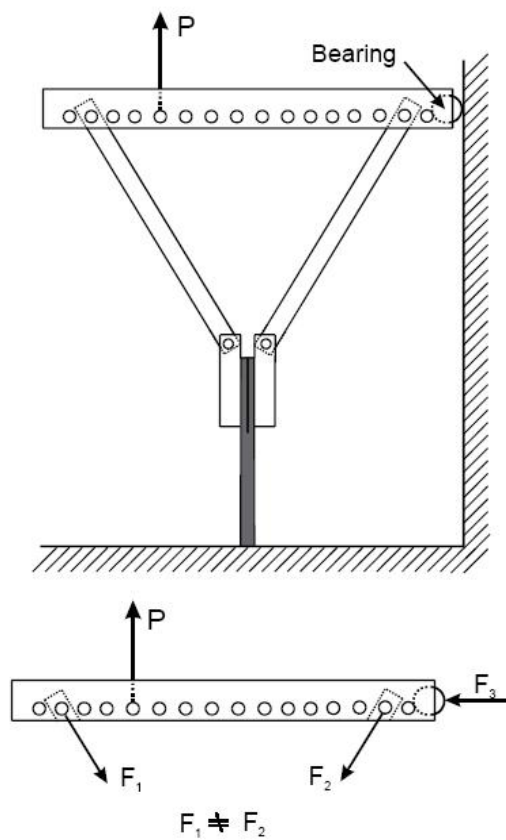


Figure 3-1: Mixed Mode testing fixture

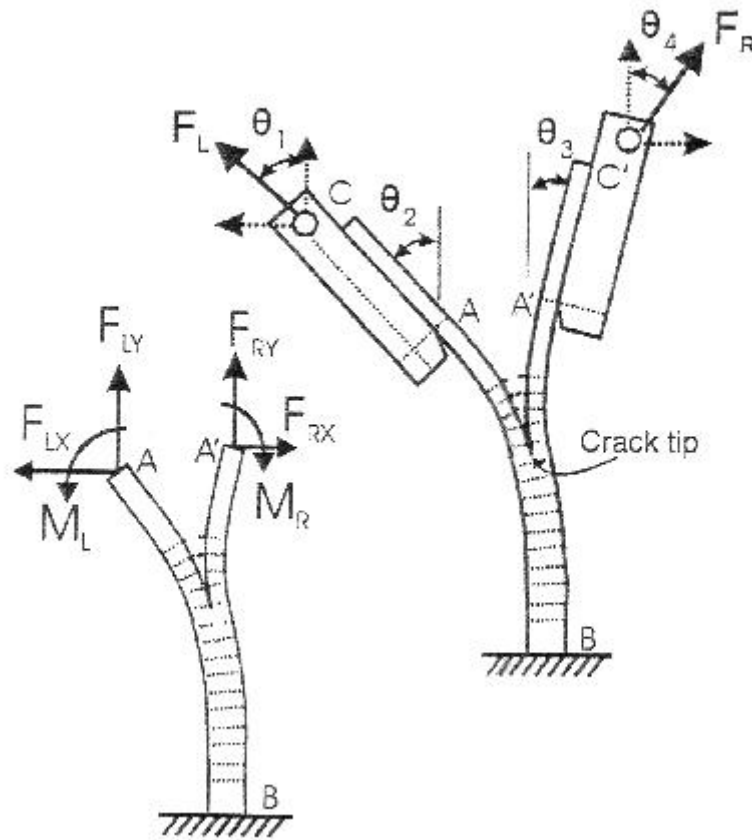


Figure 3-2: Free body diagram (FBD) of specimen showing horizontal and vertical force components

At the right end of the bar, a bearing reacts to create a horizontal force which helps balance the fixture as well as reduce compressive bending stresses that might otherwise lead to premature failure of the specimen (before stitch failure). This fixture applies tension to both arms of the DCB specimen, which also reduces the compressive bending stresses. This tensile force effectively neutralizes the compressive bending stresses in the specimen arms. By changing the loading position, various mixed mode ratios are obtained. Mode I is achieved by loading the fixture at a hole directly inline with the specimen. By offsetting the load from the longitudinal axis of the specimen, various mixed mode ratios are achieved as the ratio of forces in each loading bar is changed. In addition, the fixture can be self balanced by adding weights to the left side of the

horizontal bar to account for errors caused by the unbalanced weight of the fixture (Fig. 3-4). This fixture relies on specimen grips that can transmit both axial and transverse forces (Fig. 3-3).

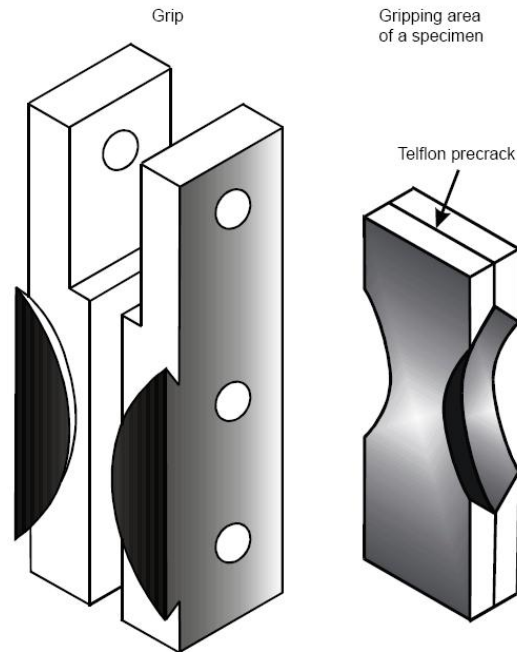


Figure 3-3: Grip and specimen ends showing machined arcs used for attachment

The transverse component of the force is for crack opening and the axial component is used to provide the tensile stresses as mentioned earlier. The conventional method of bonding tabs to the specimen does not work as the large tensile and shear stresses caused by the load required to propagate the crack simply debond the tabs. A notch in the form of a circular arc was machined in the specimen ends (Fig. 3-3). A pair of grips that match the notch profile in the specimen were machined out of steel.



Figure 3-4: Mixed Mode fixture showing counterbalance weight for balancing of mechanism prior to testing

### **Specimen Preparation**

The stitched specimens were made of 28 plies of AS4 uniweave graphite fabric and 3501-6 epoxy resin using the RTM process by NASA Langley Research Center. The specimens were stitched with 1600 denier Kevlar 29 where there are two Kevlar yarns in each stitch. In addition, each specimen consisted of three rows of stitches. The specimens were approximately 190.5 mm (7.5 inches) long and 19.05 mm (0.75 inches) wide. Two different stitch densities were used to evaluate the effects of stitch density on fracture toughness. Linear stitch densities evaluated were 5 stitches per inch (referred to as low density) and 9 stitches per inch (high density). The spacing between adjacent

rows of stitches was 5 mm (0.2 inch). Typically stitch density is defined as the number of stitches per square inch. This is represented by the stitching pattern, which is: (number of stitches per inch)  $\times$  (spacing between two adjacent stitch lines). Therefore the stitch densities evaluated were  $5 \times 1/5$  and  $9 \times 1/5$ . Refer to Figure 3-5. Additionally, the top and bottom plies of the specimen were covered with 1 layer of plane weave fiberglass cloth to act as a retainer for the stitches. The specimens also included a Teflon insert either 65 mm (2.55 in.) or 90 mm (3.55 in.) in length that created the pre-crack needed for crack propagation (Figs.3-3 and 3-5). The pre-crack started at the machined end of the specimen and continued up to the first row of stitches. The specimen was made up of 4 stacks where each stack consisted of 7 plies, which were oriented at  $[45^\circ/-45^\circ/0^\circ/90^\circ/0^\circ/-45^\circ/45^\circ]$ . The materials used in each stack have slightly different properties (Tables 3-1 and 3-2).

Table 3-1: Material properties for AS4/3501-6 graphite/epoxy

MATERIAL	E1 psi (GPa)	E2 psi (GPa)	$\nu_{12}$	G12 psi (GPa)	G13 psi (GPa)	G23 psi (GPa)
AS4-3501-00	15.3 e6 (105)	1.6 e6 (11)	0.34	0.8 e6 (6)	0.8 e6 (6)	0.52 e6 (3.6)
AS4-3501-45	15.04 e6 (103)	1.6 e6 (11)	0.34	0.8 e6 (6)	0.8 e6 (6)	0.52 e6 (3.6)
AS4-3501-90	14.88 e6 (102)	1.6 e6 (11)	0.34	0.8 e6 (6)	0.8 e6 (6)	0.52 e6 (3.6)

Table 3-2: Variation in thickness of each layer in the stacking sequence

PLY NUMBER	THICKNESS in. (mm)	ORIENTATION (DEGREE)	MATERIAL NAME
1	0.00633 (0.16)	45	AS4-3501-45
2	0.00633 (0.16)	- 45	AS4-3501-45
3	0.01285 (0.32)	0	AS4-3501-00
4	0.007018 (0.18)	90	AS4-3501-90
5	0.01285 (0.32)	0	AS4-3501-00
6	0.00633 (0.16)	- 45	AS4-3501-45
7	0.00633 (0.16)	45	AS4-3501-45

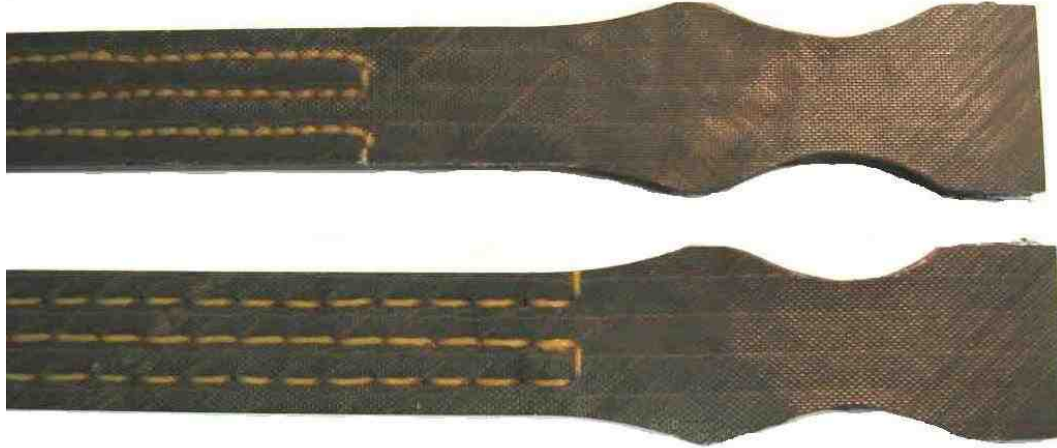


Figure 3-5: Specimens showing stitch densities and pre-crack lengths

### **Experimental Method**

Many experimental techniques are available for determining the fracture toughness of laminates. The double cantilever beam (DCB) test was chosen to accurately determine the fracture toughness of the stitched composites due to its simplicity. The DCB test consists of a specimen prepared with an initial crack length at the interface of which the fracture toughness is of interest. Tests were conducted in a screw driven universal testing machine (MTI). The crack propagation was observed using a CCD camera. A computer monitored and recorded both force and crosshead displacement. The crack propagation length was measured using a micrometer. Once the data was taken, a plot of force versus crosshead displacement was created. The area under the load deflection plot represents the work done ( $\Delta W$ ) in propagating the crack. Calculation of the fracture toughness was accomplished by dividing the work done to propagate the crack by the crack propagation length ( $\Delta a$ ) multiplied by the specimen width ( $b$ ).

$$G_{IC} = \frac{\Delta W}{b\Delta a} \quad (3-1)$$

For pure Mode I loading, the fixture is setup with the universal testing machine attached directly in line with the specimen. The load increases until the first row of stitches break, at which time the load suddenly drops (Figs. 3-6, 3-7). Subsequent rows of stitches are loaded until failure. The cycle continues in this saw tooth pattern until the specimen is unloaded. When testing stitched specimens, unloading can never be complete as the broken stitches protrude out of the newly created delamination surface and prevent the specimen from closing fully. In this case we assume that the unloading would have been elastic, and hence connect the current point on the load-deflection plot to the origin. As seen in Figure 3-6 each peak and valley corresponds to a stitch breaking. By having a peak and valley for every row of stitches in the specimen shows that the crack propagation is stable.

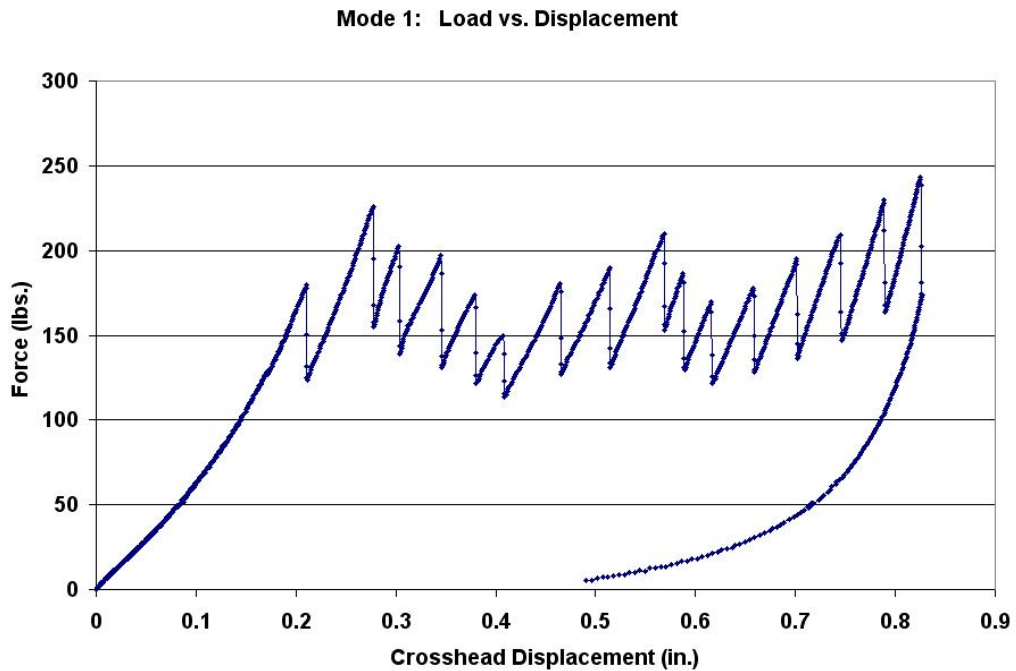


Figure 3-6: Load versus crosshead displacement plot for a stitched specimen

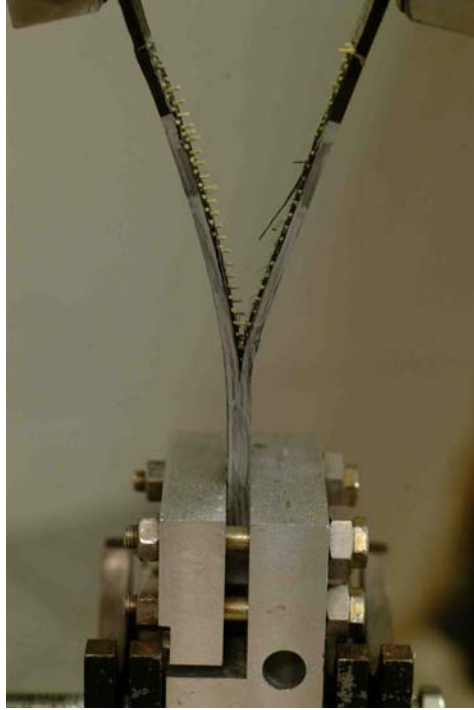


Figure 3-7: Stitched DCB specimen undergoing testing

The same procedure described for Mode I was used for mixed mode loading. To achieve various mixed mode ratios the MTI machine was attached to the horizontal bar offset from the specimen. The larger the offset the greater the mixed mode ratio becomes. The average fracture toughness values for both the low-density and high-density stitched composites are listed under Tables 4-1 and 4-2 in Chapter 4. The Mode Mixity parameter ( $\Psi$ ) defined as follows is used to describe the mixed mode ratio:

$$\psi = \tan^{-1} \frac{K_{II}}{K_I} \quad (3-2)$$

where  $K_I$  and  $K_{II}$  are the Mode I and Mode II stress intensity factors, respectively. One can note that  $\Psi=0$  for pure Mode I and  $\Psi = \pi/2$  for pure Mode II. For mixed mode conditions  $0 < \Psi < \pi/2$ . The stress intensity factor approach to calculate mode-mixity is further explained in Chapter 5.

In the present work we use a simple mechanics of materials approach to estimate the mode-mixity  $\Psi$ , which is based on the ratio between the forces transmitted to the

specimen in each bar of the fixture. We calculate both  $G_I$  and  $G_{II}$  (energy release rates) based on strength of material calculations (Fig. 3-8 and Eq. 3-3) and use the superposition of the symmetric and anti-symmetric loads to calculate  $\Psi$ . The energy release rates are proportional to the square of the stress intensity factors. Therefore, the energy release rates are calculated and then converted to stress intensity factors values, which are then used in Equation 3-2 to calculate  $\Psi$ .

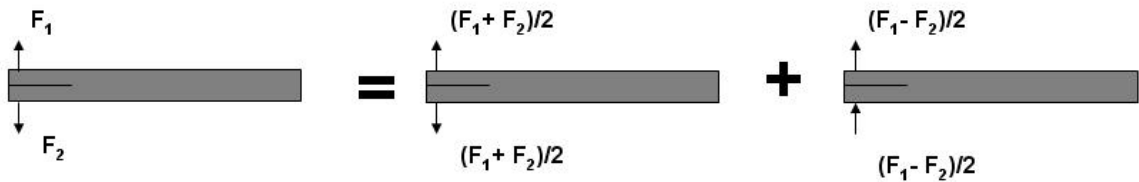


Figure 3-8: Schematic of forces for strength of material calculations

$$\frac{G_{II}}{G_I} = \frac{3}{4} \left( \frac{1 - \frac{F_2}{F_1}}{1 + \frac{F_2}{F_1}} \right)^2 \quad (3-3)$$

## CHAPTER 4 FRACTURE TESTS

### **Introduction**

As explained previously the fracture toughness ( $G_c$ ) of a material can be described or defined as the energy needed to initiate crack propagation. Fracture toughness is a material property and therefore should remain constant under a given loading condition. Typical  $G_c$  values for a graphite/epoxy laminate are on the order of 300 J/m<sup>2</sup> (1.7 lbin/in<sup>2</sup>) for Mode I delamination crack propagation. Previous research has shown that the addition of stitches increases the fracture toughness significantly especially under Mode I loading conditions. This is most likely due to the fact that stitches are primarily effective in tension rather than shear.

### **Testing and Discussion**

As previously discussed the specimens were tested using an MTI machine configured with the test fixture described in the previous chapter. Both low stitch-density and high stitch-density specimens were tested. For the high-density specimens, the fixture was adjusted by moving the arms inward toward the loading attachment point. This increases the tension force in each arm, effectively reducing the compressive bending stresses, which cause specimen breakage.

Average apparent fracture toughness for both low-density and high-density specimens can be found in Tables 4-1 and 4-2 respectively.

Table 4-1: Average apparent fracture toughness of low-density stitched specimens

MODE RATIO $\Psi = \tan^{-1} (K_{II}/K_I)$	AVERAGE G lb-in/in <sup>2</sup> (J/m <sup>2</sup> )
0°	40.45 (7083)
8.2°	36.27 (6351)
16.0°	43.16 (7557)
29.9°	46.60 (8160)

Table 4-2: Average apparent fracture toughness of high-density stitched specimens

MODE RATIO $\Psi = \tan^{-1} (K_{II}/K_I)$	AVERAGE G lb-in/in <sup>2</sup> (J/m <sup>2</sup> )
0°	81.80 (14323)
12.1°	96.80 (16950)
23.3°	100.74 (17640)
29.9°	-

As the mixed mode ratio increases from Mode I to Mode II the apparent fracture toughness value increases significantly over that of an unstitched specimen and remains fairly constant over the mixed mode range with a decrease most likely appearing near the pure Mode II loading condition.

One may notice that no fracture toughness value can be found for high-density specimens above the mixed mode ratio of 23.3°. This is due to the fact that at mixed mode ratios higher than this, the specimen would break either from compressive breakage in one of the arms or in shear at one of the end grips.

Figure 4-1 shows a plot of the fracture toughness versus the mode-mixity angle for low-density stitched specimens. A linear trend line has been fitted to the experimental data to show the trend of the fracture toughness with respect to the mode-mixity angle. As the mode-mixity angle increases there is a slight increase in the fracture toughness value over a 30° mode-mixity range. The Mode II (90°) fracture toughness value was found for a stitched specimen using an End-Notch-Flexure test by Chen et al. [6]. The

dotted trend line is shown as an illustration that the fracture toughness will eventually decrease to the Mode II value. The exact shape of this trend line between 30° and 90° (dashed line in Fig. 4-1) at the present moment is unknown.

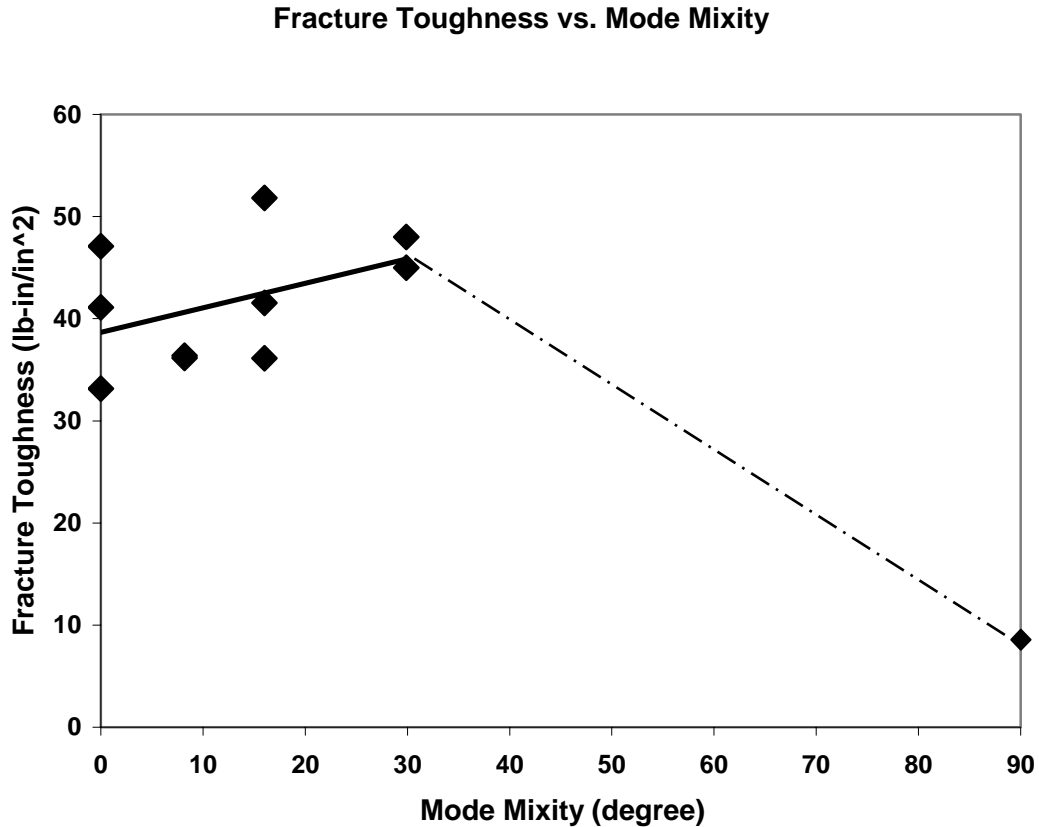


Figure 4-1: Fracture toughness versus mode-mixity over entire Mode I to Mode II range

The force versus crosshead displacement data collected from the MTI machine is shown in Figures 4-2 thru 4-9.

Shown in Figure 4-2 is the load versus crosshead displacement for a Mode I loading done on three low density specimens. As one can observe, there is some non-linearity to both the loading and unloading of the specimen. Additionally, one of the specimens has a different loading slope curve. This is due to stitches starting further down on that specimen compared to the other two specimens (Refer to chapter 3).

Specimens with a pre-crack length of both 65 mm (2.55 in.) and 90 mm (3.55 in.) were tested. Due to this fact the loading curves will have slightly different shapes.

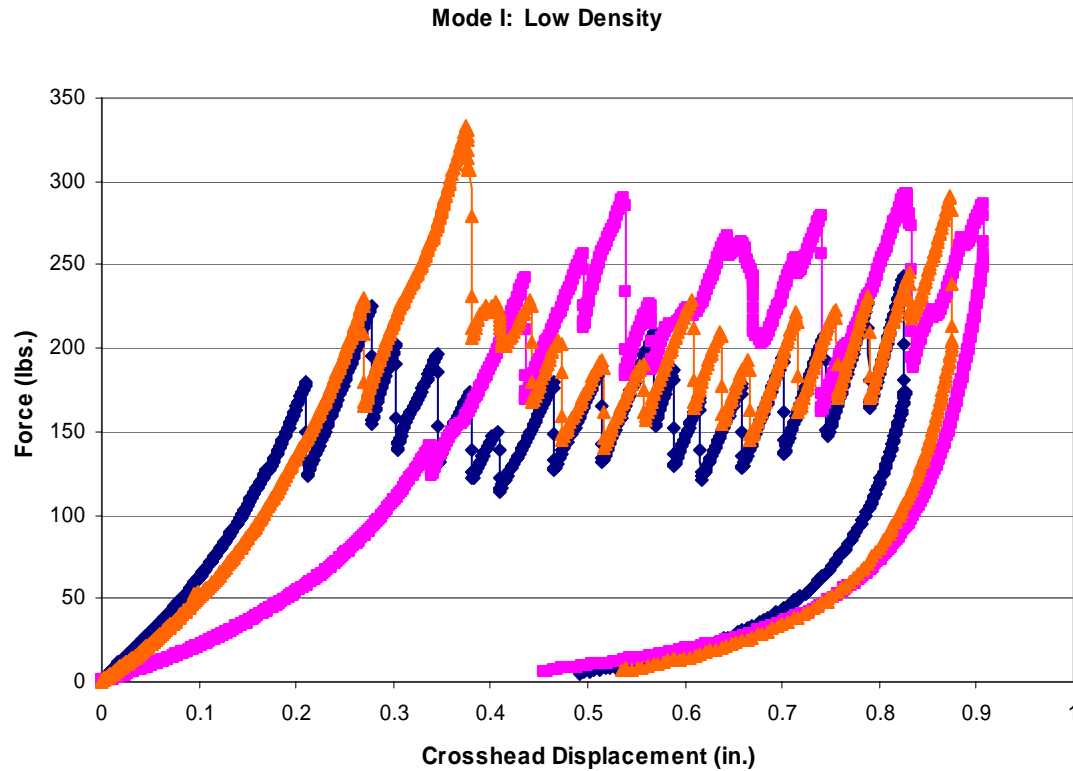


Figure 4-2: Mode I loading: low density specimens, load vs. crosshead displacement

Figure 4-3 shows the load versus crosshead displacement curve for a mixed mode loading of  $8.2^\circ$  on two low density specimens. There is slightly more non-linearity under the mixed mode loading compared to that of the Mode I loading. Very good repeatability between the two specimens can be observed. Notice that each peak and valley corresponds to a row of stitches breaking, meaning the crack propagated in a stable manner. By the crack propagating in a stable manner the analysis of the fracture toughness can more easily be performed. Meaning that for each stitch breaking there is crack length that corresponds to the breakage.

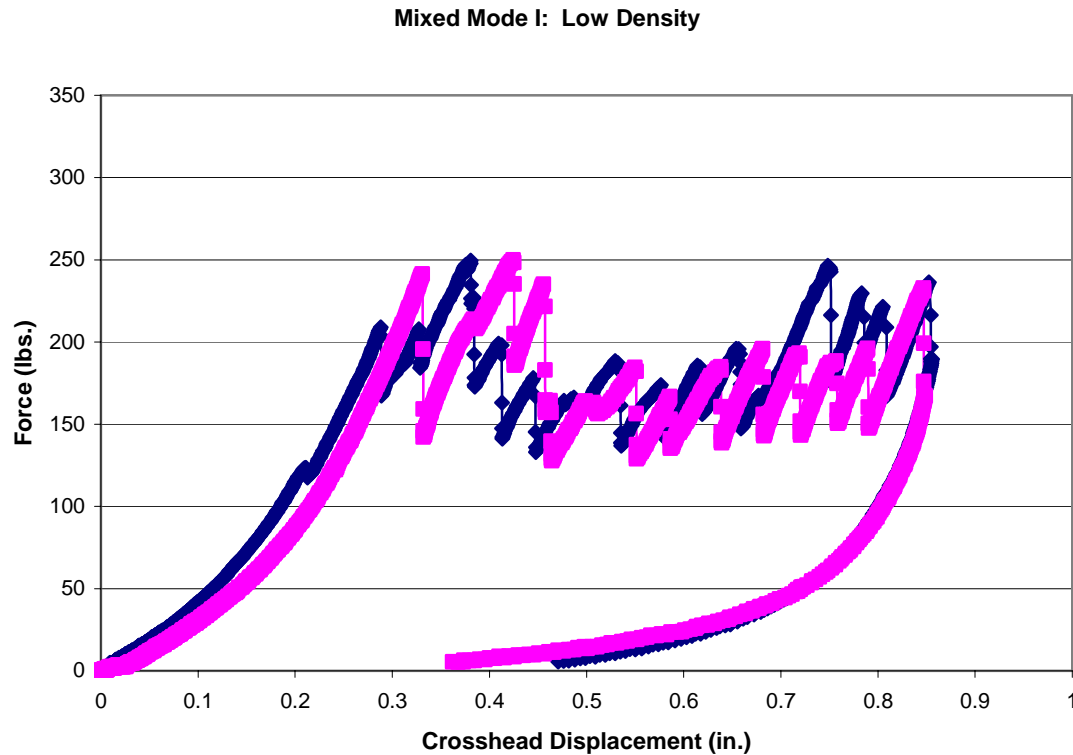


Figure 4-3: Mixed Mode 1 loading: low density specimens, load vs. crosshead displacement

Figure 4-4 shows the load versus displacement curve for a mixed mode loading of  $16.0^\circ$  for low density specimens. The non-linearity of the initial load buildup grows even greater when compared to the previous two loading conditions. The average force for stitch breakage and crack propagation has increased from approximately 200 lb. (890 N) to 250 lb. (1100 N). Additionally, it can be observed that the force needed for stitch breakage has quite a large (up to 45% difference) variation between specimens.

Figure 4-5 shows the load versus displacement curve for a mixed mode loading of  $29.9^\circ$  for low density specimens. These specimens have a very non-linear initial loading curve. Also, it is important to point out that on one of the specimens, crack propagation was unstable as there was a large peak load which broke a number of rows of stitches at once. This can easily be seen as one specimen does not have nearly as many peaks and

valleys as the other. Notice the drastic increase in average stitch breaking force when compared to the previous three loading conditions. This shows that as the mixed mode ratio increases the force needed to break stitches and propagate the crack increases. This is very important because specimen breakage can occur if this force gets too large.

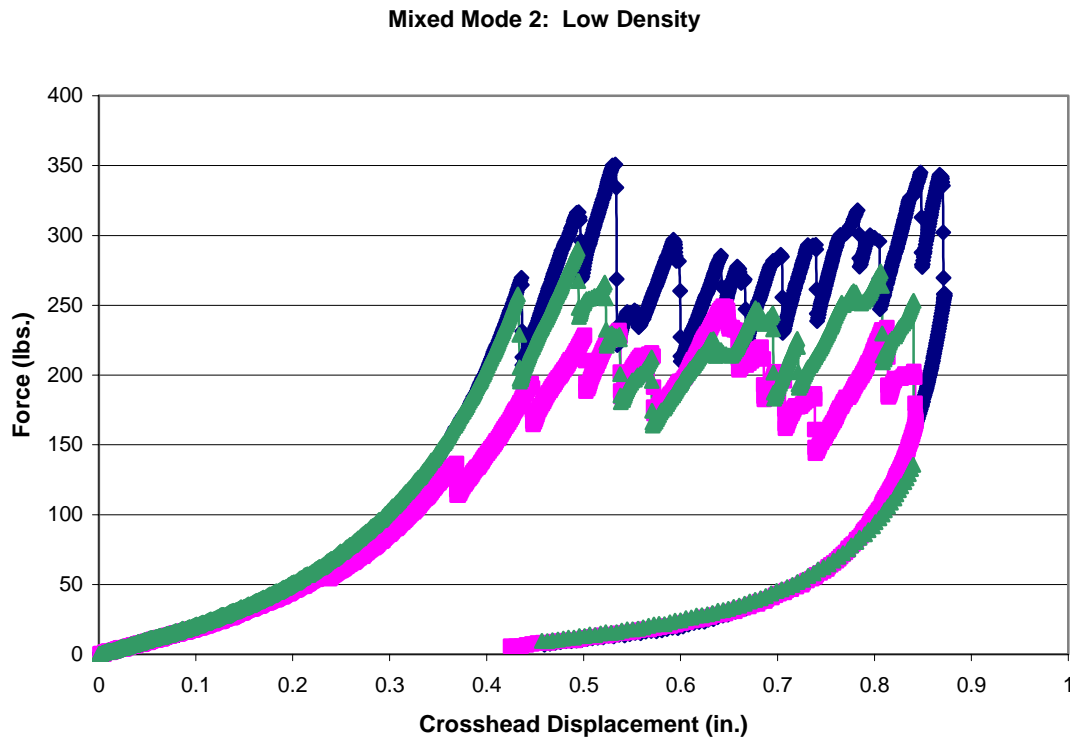


Figure 4-4: Mixed Mode 2 loading: low density specimens, load vs. crosshead displacement

Figure 4-6 shows the load versus displacement curve for a mode I loading on high density specimens. When compared to the low density specimens, it can be observed that the average force for crack propagation has increased significantly to an average force of approximately 550 lb. (2400 N). Because these specimens are stitched more densely, the number of peaks and valleys has increased.

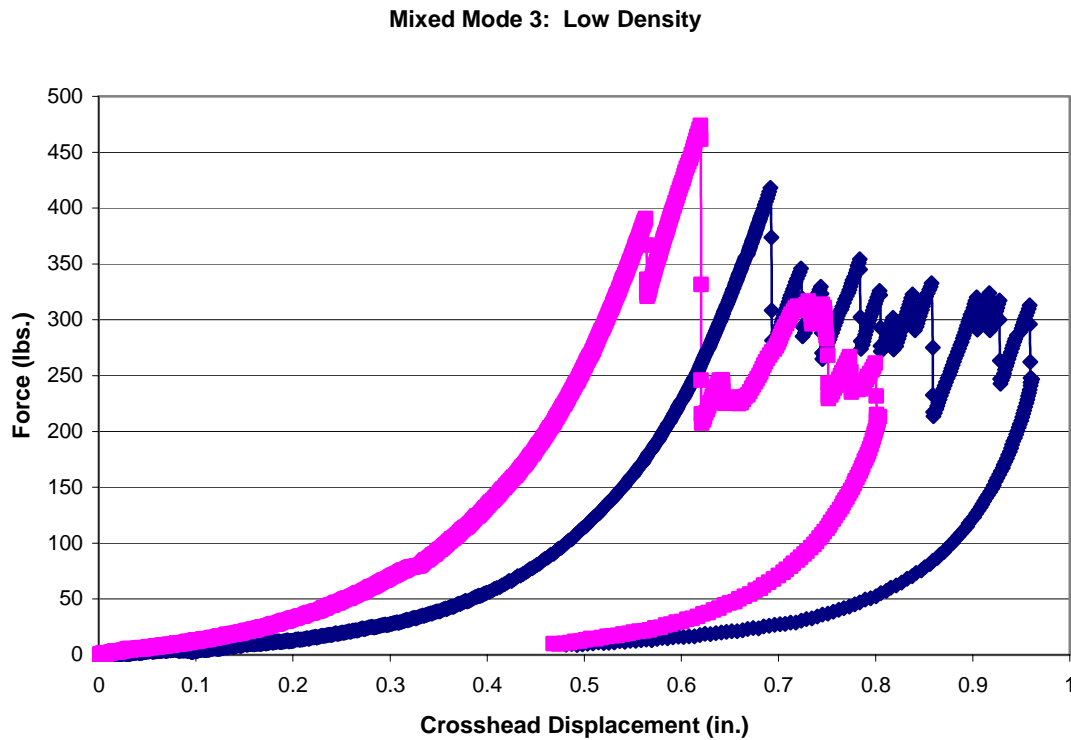


Figure 4-5: Mixed Mode 3 loading: low density specimens, load vs. crosshead displacement

Figure 4-7 shows the load versus displacement curve for a mixed mode loading of  $12.1^\circ$  for a high density specimen. Notice the increase in non-linearity on the loading curve and the large increase in stitch propagation force. This non-linearity may be due to the complex mechanism used in the fixture. Average force is approximately 900 lb. (4000 N).

Figure 4-8 shows the load versus displacement curve for a mixed mode loading of  $23.3^\circ$  for high-density specimens. Notice that one specimen is loaded and fails due to compressive bending in the arm. After the specimen broke, the fixture was adjusted by moving the loading arms inward to increase the tensile force in each arm to aid in reducing bending stresses. The next specimen does not fail, but the crack propagates unstably as there are three peaks and valleys which correspond to approximately 15 rows

of stitches breaking. Also, the average crack propagation force has increased once again to approximately 2000 lb. (8900 N), which is an increase of almost 1100 lb. (5000 N) from the previous loading condition.

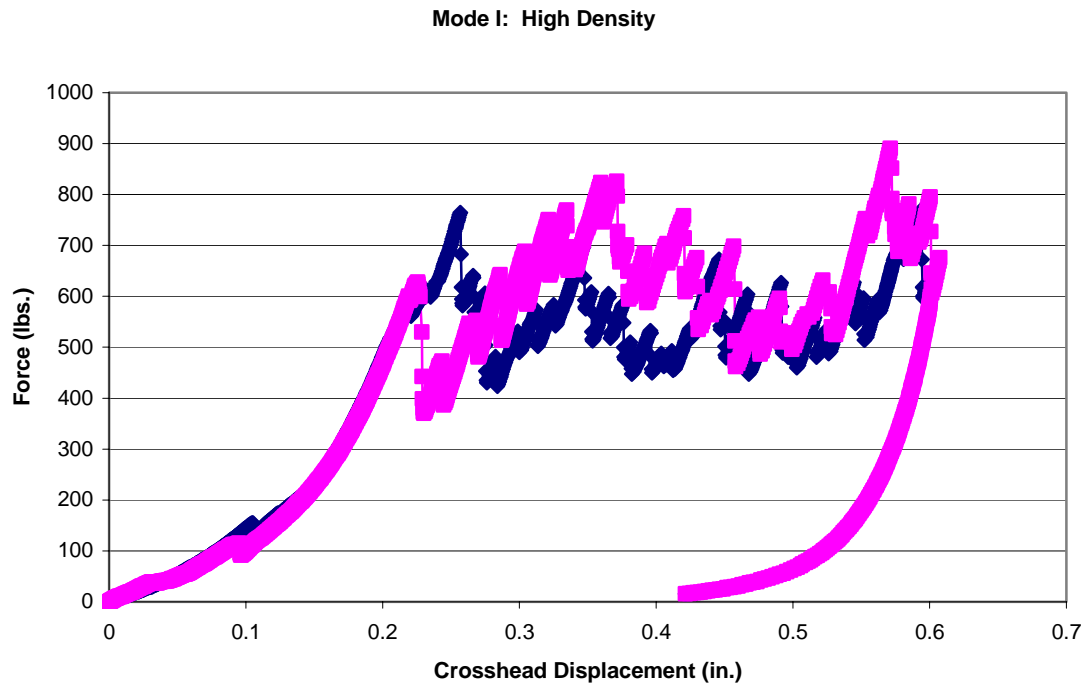


Figure 4-6: Mode I loading: high density specimens, load vs. crosshead displacement

Figure 4-9 shows the load versus displacement curve for a mixed mode loading of  $29.9^\circ$  for a high density specimen. Notice that the specimen is unable to open and breaks due to shearing at the grip attachment point. Testing highly stitched specimens is an intricate process and refinement to the testing fixture or a new fixture must be developed in order to test specimens such as these.

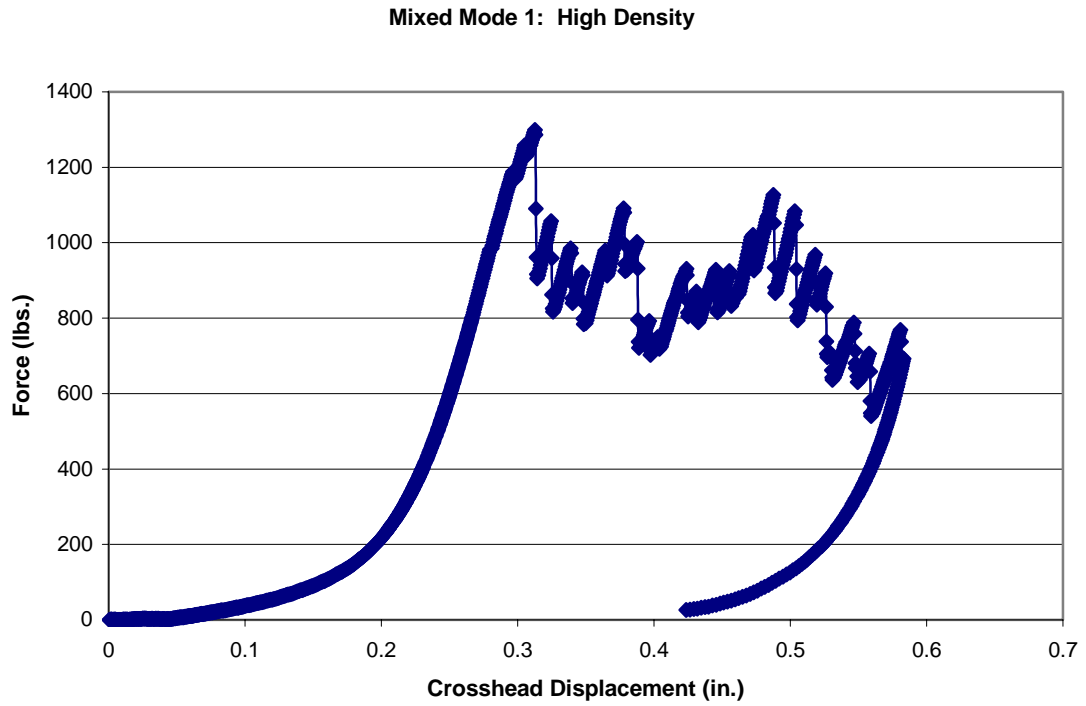


Figure 4-7: Mixed Mode 1 loading: high density specimens, load vs. crosshead displacement

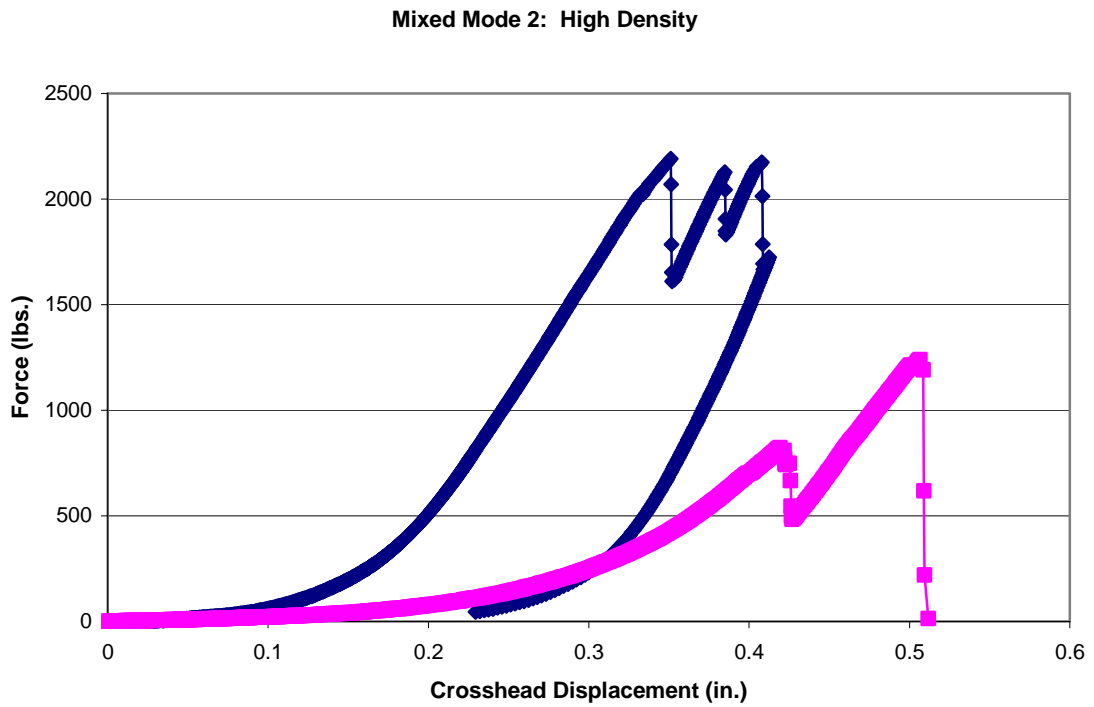


Figure 4-8: Mixed Mode 2 loading: high density specimens, load vs. crosshead displacement

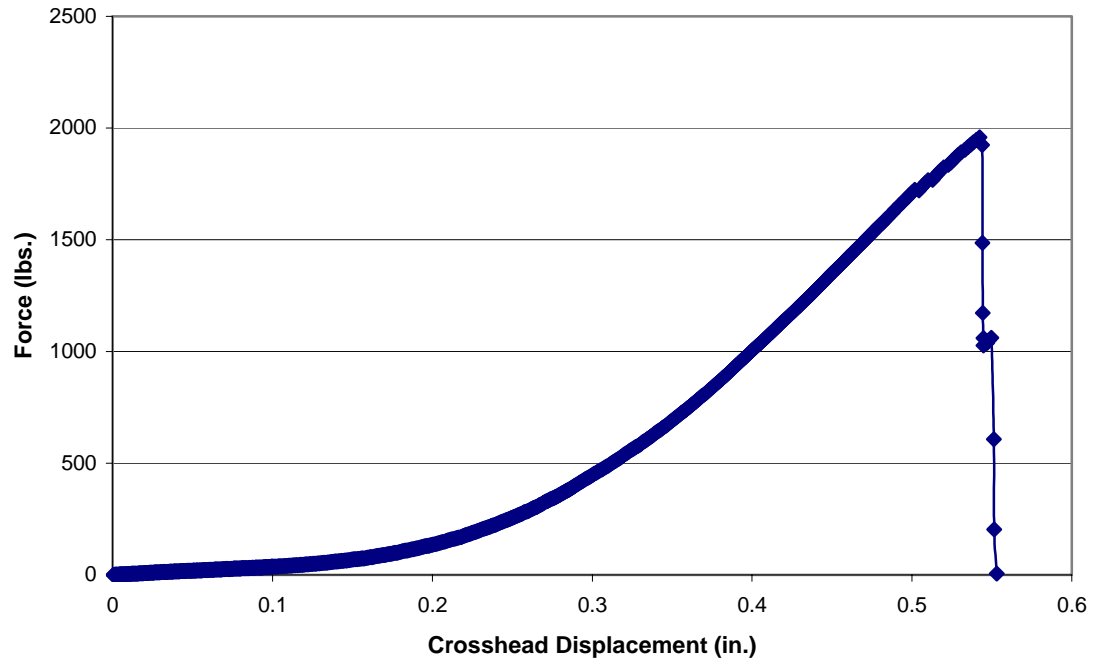
**Mixed Mode 3: High Density**

Figure 4-9: Mixed Mode 3 loading: high density specimens, load vs. crosshead displacement

## CHAPTER 5 FINITE ELEMENT ANALYSIS

### **Introduction**

To better investigate and understand the mechanics of the loading fixture and the stitched laminate, a finite element (FE) model was created. This model would allow for the investigation of the stitch interactions with the parent laminate and investigation of stitch failure mechanisms. Additionally, in the FE model the material properties of the laminate, including the stitch material, stitching density, and stitch diameter, could be varied in order to quickly evaluate the sensitivity of fracture toughness with respect to these parameters. By modeling the entire loading fixture instead of just the stitched laminate, the mode-mixity could be evaluated at the crack tip under a given loading arrangement as described in the previous sections. This would allow verification of the experimental setup.

The FE simulation was performed using a two dimensional (2D) model to exploit mechanical symmetry, and also to minimize required computation time. Data gathered from experimentation was directly incorporated into the model. Specifically, the entire specimen geometry and ultimate failure loads were incorporated in the model to ensure its representation of the physical test setup. The FE model was created with a goal of extracting stresses in the laminate and forces transmitted through the loading fixture. In particular, the strain energy release rate, stresses at the crack tip and the strain in the stitches were of interest. The J-integral was used to calculate  $G_{\text{parent}}$  (strain energy release rate of the parent material) by using a contour which did not include the stitches.  $G_{\text{eff}}$

(effective strain energy release rate) was also evaluated by using a contour that circumvented the stitches in the laminate.  $G_{\text{parent}}$  is a material property of the parent laminate while  $G_{\text{eff}}$  depends on both the properties of the laminate and the properties of the stitches.

### **Procedure of Modeling**

The first step in the modeling process was to create the DCB specimen. This was done by creating each individual half of the specimen and then attaching the halves in such a way that a pre-crack was created down the centerline of the model, mimicking the Teflon insert on the physical model. Appropriate orientation-dependent material properties were assigned to individual layers. The elements used for the laminate were planar (plane stress) 2D elements. After the model was assembled, the next step was to add the stitches to the specimen. The stitches were modeled as truss elements, which were attached by sharing nodes at the very top and bottom of the laminate. This does not completely characterize how the stitches are truly attached within the physical model but can be assumed a close approximation. The stitches were assigned isotropic material properties of Kevlar 29. The stitches were estimated as having a circular cross-section with the diameter being calculated by knowing that Dupont™ Kevlar 29 yarns have a denier of 1600. Next, the grips were modeled and attached to the laminate, making sure that all dimensions are representative of the physical setup. Finally, beam elements were used to model both the top and side bars of the fixture. The beams were assigned the material properties of steel and the dimensions of the physical model. Careful attention during the assembly was needed to ensure that no degrees of freedom were constrained unintentionally. The FE model can be seen in Figures 5-1 and 5-2.

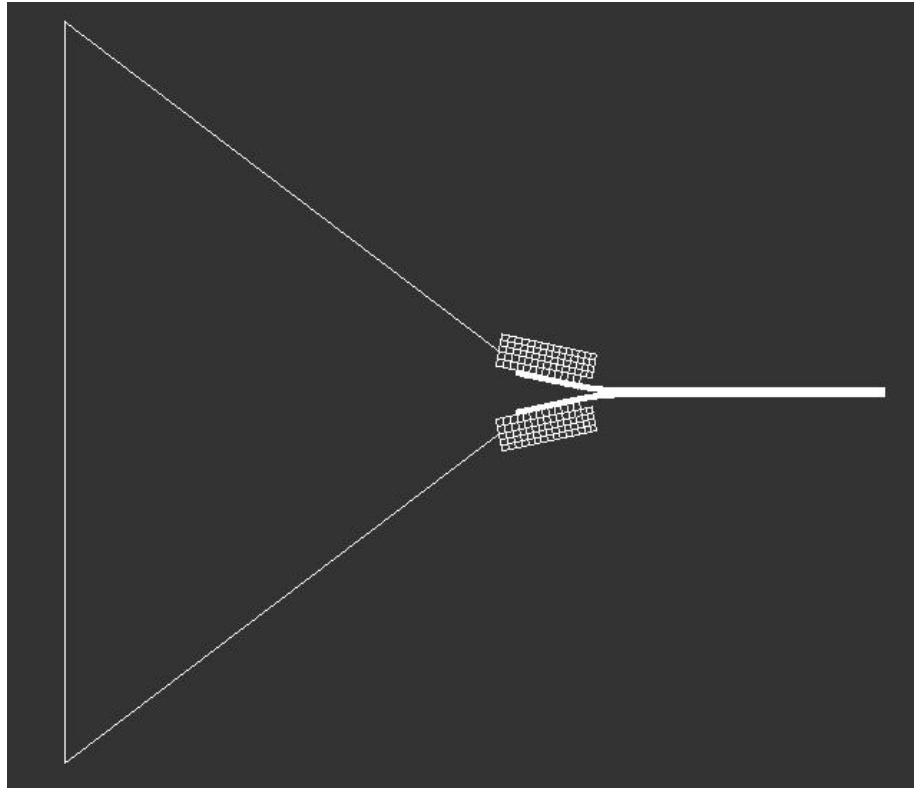


Figure 5-1: 2D FE model of fixture and laminate

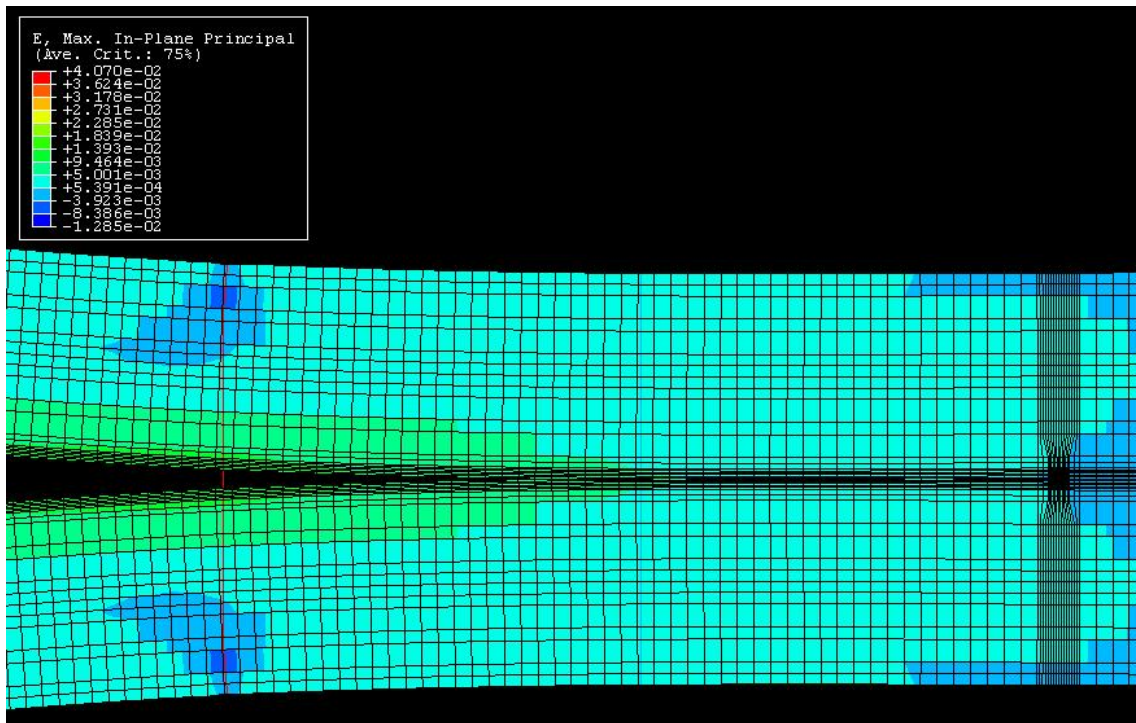


Figure 5-2: FE model showing crack tip and stitches including the stitch bridging distance

### Modeling Results

The J-Integral approach was used to gather both the  $G_{\text{parent}}$  and  $G_{\text{eff}}$  from the FE models. Each model was loaded with the ultimate failure load of the stitches as measured from experimental testing. Then the G values were recorded at the crack tip. The J-Integral approach in the ABAQUS FE software returns a plot of contour number versus strain energy release rate. An example of this chart is shown in Figure 5-3. One can observe that near the crack tip the strain energy release rate is approximately 2 lb-in/in<sup>2</sup> (350 J/m<sup>2</sup>) which is very representative of the actual fracture toughness value of a graphite/epoxy laminate. Also, it can be seen that once the contour grows large enough to include the stitch the strain energy release rate increases to a value of about 53 lb-in/in<sup>2</sup>, which is similar to the experimental fracture toughness values. The G values are found in Table 5-1. The importance here more than the actual number values is the trend of both  $G_{\text{parent}}$  and  $G_{\text{eff}}$ .  $G_{\text{parent}}$  increases as the mode-mixity increases, which agrees with conventional theory. On the other hand  $G_{\text{eff}}$  remains fairly constant over the mixed mode loading range. This matches the trend observed during experimental testing.

Table 5-1: FE parent and effective fracture toughness

Specimen ID (Low Density)	FEM Parent $G$ lb-in/in <sup>2</sup> (J/m <sup>2</sup> )	FEM Effective $G$ lb-in/in <sup>2</sup> (J/m <sup>2</sup> )
Mode I	2.3 (403)	53 (9275)
Mixed Mode 1	6.5 (1138)	76 (13300)
Mixed Mode 2	15 (2625)	81 (14175)
Mixed Mode 3	22 (3850)	74 (12950)

Mode I: Strain Energy Release Rate vs. Contour Number

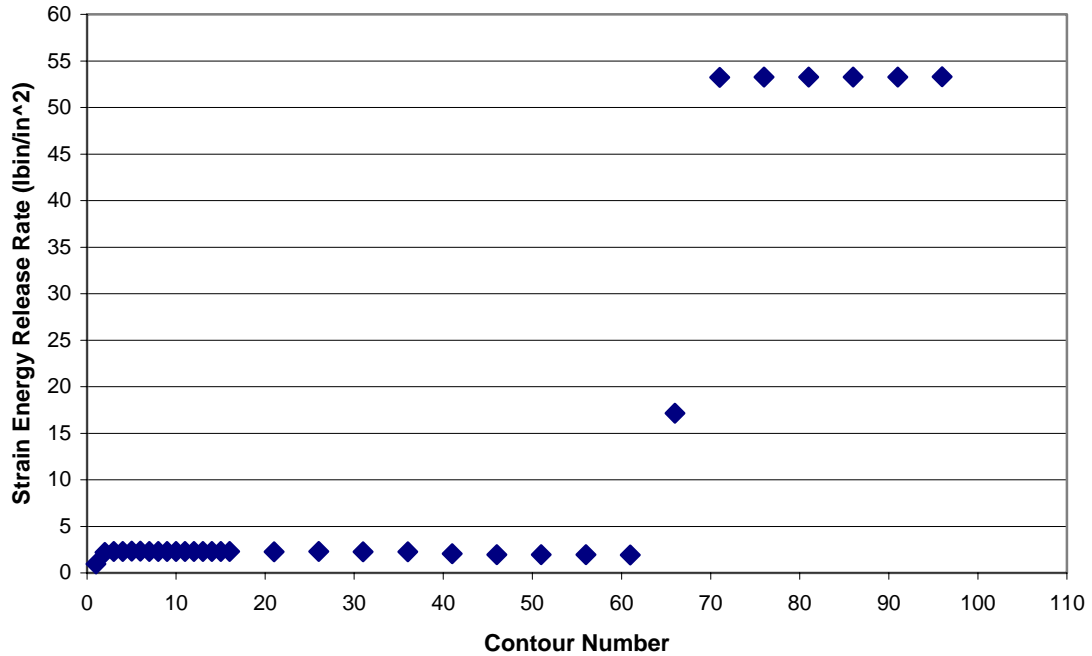


Figure 5-3: Strain energy release rate versus J-Integral contour number

Additionally, given the stresses incurred at the crack tip the stress intensity factors were calculated at the crack tip (Table 5-2). From the intensity factors the mixed mode ratio at the crack tip was calculated.

$$T = \tan^{-1} \frac{K_{II}}{K_I} \quad (5-1)$$

This local mixed mode ratio ( $T$ ) is significantly different from the global mixed mode ratio ( $\Psi$ ) of which the fixture was loaded. This may be due to the fact that the stitches act as a shield, which effectively modifies the loading at the crack tip, such that the local-stress state defining local mode-mixity is different from the global mode-mixity defined by the fixture loads. The stitch acts like a cable which carries the Mode I loading, while allowing the shear stress from the Mode II loading to transfer to the crack tip. Table 5-3 shows a comparison of the global mixed mode ratio to the local mixed

mode ratio. Further research in this area should be conducted. Experimental work needs to be done to further characterize the movement of the stitches through the parent laminate. From this research further refinement of the FE model could be done which could verify the possibility of the two different mixed mode ratios occurring in stitched composites.

Table 5-2: Stress intensity factors at crack tip

Specimen ID (Low Density)	$K_I$ psi- $\sqrt{\text{in}}$ (MPa- $\sqrt{\text{m}}$ )	$K_{II}$ psi- $\sqrt{\text{in}}$ (MPa- $\sqrt{\text{m}}$ )
Mode I	2472.9 (2.7)	136.7 (0.15)
Mixed Mode 1	2686.9 (2.95)	2274.2 (2.5)
Mixed Mode 2	2545.0 (2.8)	4702.4 (5.2)
Mixed Mode 3	2066.9 (2.3)	6773.2 (7.4)

Table 5-3: Global versus local mode-mixity ratios

Specimen ID (Low Density)	Global Mode Mixity ( $\Psi$ )	Local Mode Mixity (T)
Mode I	0°	3°
Mixed Mode 1	8.2°	40°
Mixed Mode 2	16.0°	61°
Mixed Mode 3	29.9°	74°

### Crack Propagation Model

To simulate the experimental testing that was performed, a crack propagation model was created. Initially a given crack length and bridging length is chosen. The model is loaded and both the strain in the stitches and the energy release rate of the parent material is monitored. If the strain in the stitches exceeds the failure strain (4%) then the stitch is considered broken and removed from the model. Additionally, if the strain energy release rate of the parent material exceeds the critical fracture toughness value the crack is allowed to propagate. Then this procedure repeats itself. The modeling process is an iterative one in which the strain and energy release rate are continuously being measured and compared to the critical values. A linear assumption was used in creating this model. Therefore the model will not mimic the experimental results perfectly. The

data collected in simulating the loading and failure of one stitch is shown in Table 5-4. Additionally, Figure 5-4 shows the plot created from this model showing the first stitch failure.

There is a close agreement between this crack propagation model and the experimental results which were gathered for a Mode I low density specimen. Failure occurs at approximately a load of 225 lb. (1000 N) in both cases. The displacement in the crack propagation model is greater than the experimental case, but this is due to the fact that the crack propagation model used a linear assumption which did not incorporate any non-linear effects. Additionally, the load drop after stitch failure is very similar to that of the experimental case.

Table 5-4: Data needed to simulate crack propagation

Crack Length from specimen edge in. (mm)	Crack Length from leading stitch in. (mm)	Displacement in. (mm)	Load lb. (N)	G lb-in/in <sup>2</sup> (J/m <sup>2</sup> )	Stitch Strain
2.55 (64.8)	0	0.318 (8.1)	225 (1000)	45.5 (7963)	0.006
2.634 (66.9)	0.084 (2.1)	0.345 (8.8)	225	27 (4725)	0.0229
2.717 (69.0)	0.167 (4.2)	0.357 (9.1)	225	8.5 (1488)	0.037
2.8 (71.1)	0.25 (6.4)	0.361 (9.2)	225	1.1 (193)	0.0423
2.884 (73.3)	0.334 (8.5)	0.3655 (9.3)	225	0.02 (3.5)	0.0466
2.967 (75.4)	0.417 (10.6)	0.3644 (9.25)	225	1.17 (204)	0.0462
3.05 (77.5)	0.5 (12.7)	0.3635 (9.23)	225	2.5 (438)	0.0407
3.05* (77.5)	0.5 (12.7)	0.438 (11.1)	225	54 (9450)	0.0067
3.133* (79.6)	0.583 (14.8)	0.472 (12.0)	225	34 (5950)	0.026
3.217* (81.7)	0.667 (16.9)	0.4875 (12.4)	225	12 (2100)	0.043
3.3* (83.8)	0.75 (19.1)	0.49 (12.45)	225	2.25 (394)	0.051

Note: \* Denotes leading stitch was removed from FE model to simulate stitch failure

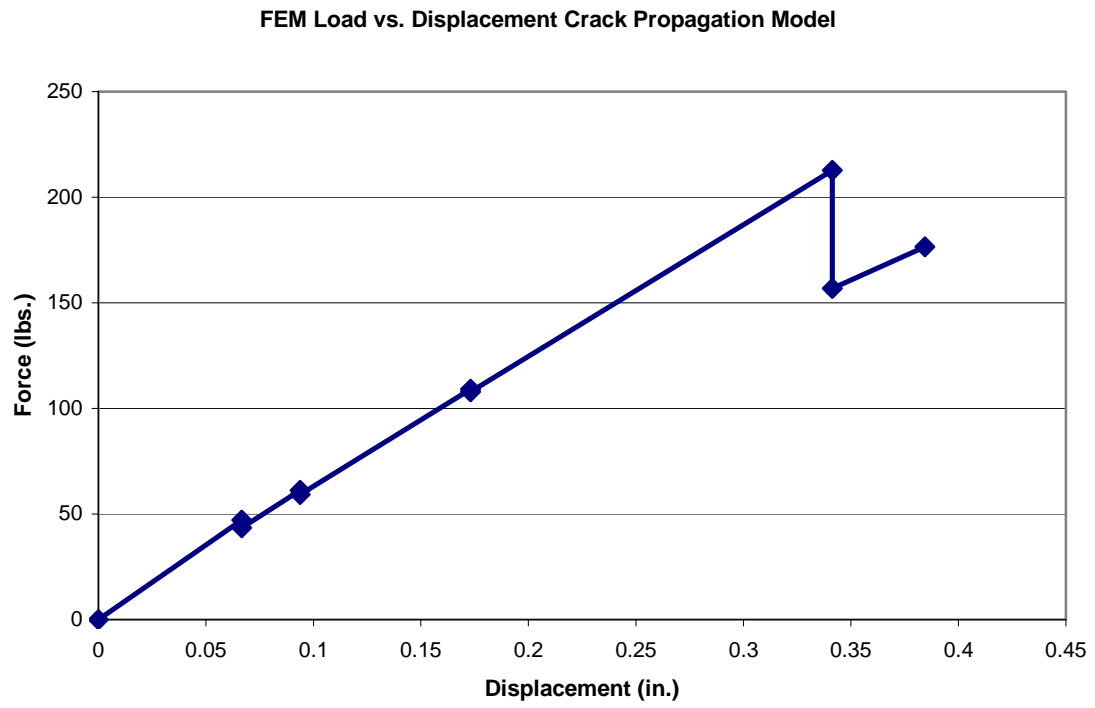


Figure 5-4: Crack propagation model showing first stitch failure

## CHAPTER 6 CONCLUSIONS

### Summary

The research presented in this thesis is an effort to better understand the failure phenomenon in laminated composites that are reinforced through their thickness with stitches. Through-the-thickness stitching is a method that increases translaminar strength while at the same time preventing crack propagation. The fracture toughness of stitched composites was evaluated under combined Mode I and Mode II loadings (known as mixed-mode loading). Additionally, a finite element (FE) model was created to be able to rapidly study the effects of stitching on a laminate under numerous loading conditions.

### Conclusions

As a result of this study, the following conclusions were reached.

1. Stitching effectively increases the apparent fracture toughness of stitched composites. The increase is on the order of 20 fold for low-density stitched specimens and 40 fold for high-density stitched specimens.
2. For the limited global mode-mixity ( $\psi$ ) range observed ( $0^\circ < \psi < 30^\circ$ ), the apparent fracture toughness  $G_c$  seems to increase slightly with increasing  $\psi$ . This agrees with theory as stitches are most effective in tension and keep the fracture toughness value fairly constant.
3. FE models can be used to accurately simulate the crack propagation in stitched composites. From these models, the material properties and physical dimensions of both the parent laminate and stitch can be varied to see what effect these changes have on apparent fracture toughness.
4. The J-Integral approach can be effectively implemented to evaluate stitched composites. Care should be taken to make sure that the contour either includes or excludes the stitches depending if one is interested in the value of  $G_{\text{parent}}$  or  $G_{\text{eff}}$  respectively.

5. Local and global mode-mixity ratios are not the same for stitched composites. The stitches effectively modify the loading condition by carrying the tensile forces while allowing the shearing forces to transfer to the crack tip. Thus, resulting in higher mixed mode ratios at the crack tip.

## LIST OF REFERENCES

1. Mignery LA, Tan TM and Sun CT. "The Use of Stitching to Suppress Delamination in Laminated Composites", ASTM STP 876, American Society for Testing and Materials, 1985, pp 371-385.
2. Dexter HB and Funk JG. "Impact Resistance and Interlaminar Fracture Toughness of Through-the-Thickness Reinforced Graphite/Epoxy," AIAA paper 86-1020-CP, 1986 pp 700-709.
3. Ridards R and Korjakin A. "Interlaminar Fracture Toughness of GFRP Influenced by Fiber Surface Treatment," Journal of Composite Materials, Vol. 32, No. 17, 1998, pp 1528-1559.
4. Reeder JR and Crews JH Jr. "Mixed Mode Bending Method for Delamination Testing," AIAA paper Vol. 28, No. 7, Jul. 1990, pp 1270-1276.
5. Reeder JR and Crews JH Jr. "Redesign of the Mixed Mode Bending Delamination Test to Reduce Nonlinear Effects," Journal Composites Technology and Research 1992 pp 12-18.
6. Chen L, Sankar BV and Ifju PG. "Mixed Mode Fracture Toughness Tests for Stitched Composite Laminates," AIAA paper 2003-1874, 2003 CD Rom.
7. Anderson TL. Fracture Mechanics: Fundamentals and Applications, Second Edition, CRC Press, Boca Raton, FL 1995.
8. Sharma SK and Sankar BV. "Effects of Through The Thickness Stitching on Impact and Interlaminar Fracture Properties of Textile Graphite/Epoxy Laminates," NASA Contractor Report 195042, Feb. 1995.
9. Sankar BV and Sharma SK. "Mode II Delamination Toughness of Stitched Graphite/Epoxy Textile Composites," Journal of Composites Science and Technology, Vol. 57, 1997 pp 729-737.
10. Jain LK, Dransfield KA, and Mai YW. "On the Effects of Stitching in CFRPs-II. Mode II Delamination Toughness," Journal of Composites Science and Technology, Vol. 58, 1998 pp 829-837.
11. Gui L and Li Z. "Delamination Buckling of Stitched Laminates," Journal of Composite Science and Technology, Vol. 61, 2001 pp 629-636.

12. Yeh HY, Lee JJ and Yang DYT. "Study of Stitched and Unstitched Composite Panels Under Shear Loadings," *Journal of Aircraft* Vol. 41, No.2, March-April 2004 pp 386-392.

## BIOGRAPHICAL SKETCH

Tomek P. Rys was born in Jelenia Gora, Poland, on August 30<sup>th</sup>, 1980. He attended public schools in Manhattan, KS, for the first 18 years of his life. After graduating Manhattan High School in August 1998 he enrolled at Kansas State University (KSU). Mr. Rys studied mechanical engineering at KSU. He was actively involved in many activities while attending KSU including Pi Tau Sigma, Tau Beta Pi and Steel Ring honor societies. He also participated in societies such as S.M.E. and A.S.M.E. and was also involved in intramural sports.

After graduating from KSU in December of 2002, Mr. Rys decided to attend graduate school at the University of Florida (UF). Mr. Rys had an interest in composite materials and therefore chose solid mechanics as his area of specialization for his graduate studies. His research and focus has been presented in this thesis.

Mr. Rys graduated from UF in August 2004. Upon graduating Mr. Rys accepted a position as a composites engineer at one of the nation's largest defense contractors working on missile systems.